Creation and Improvement Principles of the Pneumatic Manual Impulse Devices

Iurii Vorobiov[1], Kateryna Maiorova[1], Iryna Voronko[1(✉)], Maksym Boiko[1], and Oleh Komisarov[2]

[1] National Aerospace University "Kharkiv Aviation Institute", 17 Chkalova Street, Kharkiv 61070, Ukraine
kate.majorova@ukr.net, i.voronko@khai.edu
[2] Motor Sich JSC, 15, Motorostroiteley Avenue, Zaporozhye 69068, Ukraine

Abstract. The aircraft structures complexity and the inaccessibility of rivets setting areas create the need for manual rivet hammers. Many developments in this area provide a wide range of tools for the assembly work. During the assembly work, the multiple-hitting pneumatic impulse hammers are used. Such kind of tools create noise and vibrations that affect a fitter. Moreover, such equipment can be used only by a highly qualified specialist. The purpose of the study is to determine the pneumatic manual impulse devices (PMID) blow energy required to auto-mate the devices design process, taking into account their design features. The engineering process of the PMID operation is simulated using the ANSYS CFX Software. For the numerical study of the problem, a system of Navier-Stokes equations is used. To determine the optimal configuration of the devices gas tracts, energy losses and stress-stain state of structural elements in their interaction, the finite element method is used. As a result of the study, the simulation with various geometry of computational domain has been carried out. The results of different approaches to reduce the calculation time when using 2D geometry are compared. Using the results of gas-dynamic calculations of the devices energy parameters, the task of designing the PMID with the required blow energy has been solved. The comparison of the simulation results made in the ANSYS CFX software with the theoretical data revealed the insignificant error, the maximum value of which is 12%. It may be caused by using many simplifications during the theoretical calculations.

Keywords: Pneumatic manual impulse device · ANSYS CFX system · Blow energy · Striker · Finite element method

1 Introduction

Basic technical requirements for the PMID are formulated according to the design analysis and experience of using assembly devices in the aviation industry [1–4]. As a result of the analysis of re-cent research and publications, it has been stated that pneumo-impulse rivet hammers PIH-90H and pneumo-impulse devices (PID) for holes mandrelling PID-90, developed at the Aircraft Manufacturing Technology department of Kharkiv Aviation

M. Nechyporuk et al. (Eds.): ICTM 2021, LNNS 367, pp. 178–191, 2022.
https://doi.org/10.1007/978-3-030-94259-5_17

Institute in the mid-1980s have proved to be the most successful in terms of design and reliable in terms of manufacturing requirements. These devices differ favorably from their analogs in improved working conditions of the operators due to minimum pressure load, minimization of the force of pressing the trigger and damping the recoil energy of the device during impact. They have higher impact energy stability due to the pressure relief valve, shut-off valve and receiver that provides the accumulation of compressed air in the required amount.

However, the existing experience of operating these models revealed a number of their short-comings. The PIH-90H crimp that has a step form to ensure self-rotation at the end of working cycle has an extremely low stability. Its best specimens made of titanium alloy Ti-5Al-5Mo-5V-3Cr (Ti5553) have maximum stability of 5–7 thousand blows. The stability of the crimps made of carbon steel W1, W108, W110, W112 and heat treated to HRC 44–46 is only 300–500 blows. Failure occurs at the point of transition from maximum diameter to minimum.

Violations of the smooth functioning of the quick release valve not only led to instability of the energy parameters of the devices, but sometimes to failures. Such a disadvantage is the most characteristic one during the long breaks in the work of PMID.

In the device design, the blow energy is regulated only by the external gearbox built into the compressed air preparation unit. Although adjusting the blow energy in this way is effective, it doesn't meet the needs for efficiency and convenience in operation. The blow energy significantly relies on the quality of the lock (the fit of the striker shank in the fluoroplastic ring), which deter-mines the pressure drop magnitude in the cavities in front of and behind the striker. Moreover, the presence of the back pressure in the cavity in front of the striker during its acceleration significantly reduces the blow energy.

In some specific cases, during the assembly in a jig, the technological operations performance by the devices with a series arrangement of the chassis and the handle (forward type) in places with constrained approaches became impossible, and therefore the pistol arrangement type of the PMID was needed.

The blow energy significantly depends on the quality of the lock (the fit of the striker shank in a fluoroplastic ring), which determines the magnitude of the pressure drop in the cavities in front of and behind the striker. The presence of back pressure in the cavity in front of the striker during its acceleration, in addition, significantly reduces the blow energy.

In some specific cases, during the assembly in a jig the performance of the technological operations by devices with a series arrangement of chassis and handle (forward type) in places with con-strained approaches became impossible, and therefore the pistol arrangement type of the PMID was asked for [5].

The blow energy damping only by a rubber damper on the tappet is also cannot be considered effective enough. The PMID reserves regarding the noise reduction parameters, ergonomic parameters, etc. are also not exhausted.

The disadvantages of PID-90 include the necessity for precise strokes coordination of the striker and mandrel with the holder and shank in the form of a rod with a flange at the end. In addition, during the forward stroke the rod will be subject to vibration and quick fatigue failure in the point of attachment to the holder due to the impulse load on the holder through the long cantilever.

In this regard, the following areas of the PMID design improvements were formulated:

- increasing the reliability of the device;
- increasing the energy stability of a single blow;
- providing the quick and convenient adjustment of the blow energy;
- extending technological capabilities of the device through the reduction of dimensional and mass parameters and new arrangement solutions;
- increasing the energy conversion efficiency of the device;
- improving hygienic and ergonomic criteria.

When implementing these improvements, the simulation of gas-dynamic processes in the PMID with finite element method (FEM) was carried out to determine the optimal configuration of the gas tracts of the devices, energy losses and stress-strain state of structural elements in their interaction.

2 Description of the Mathematical Models Applied During the Gas-Dynamic Processes Simulation in the PMID

The energy parameters of the PMID are largely determined by the gas-dynamic processes in the channels and tracts of the device, as well as conditions of energy transfer during the interaction of structural elements. Therefore, the creation of the mathematical model (MM), which allows a comprehensive description of these processes, will be especially important because it correctly predicts the blow energy, taking into account all the factors that determine the behavior of the striker and the crimp of the pneumatic tool. The ANSYS CFX system is chosen as a computer simulation system for the numerical study of the gas-dynamic processes, as its solver contains a large number of models that allow calculating the turbulent gas flow taking into account the presence of the moving solids and their interaction.

Description of the Mathematical Models Applied During the Simulation of the Gas-Dynamic Processes in the PMID. For the numerical study of this problem, a system of Navier–Stokes equations (direct numerical simulation – DNS) [6] is used, which involves the laws of conservation of mass, momentum and energy of unsteady spatial flow in the Cartesian coordinate system (x_i, $i = 1, 2, 3$):

$$\begin{aligned}
&\frac{\partial \rho}{\partial t} + \frac{\partial}{\partial x_k}(\rho u_k) = 0;\\
&\frac{\partial (\rho u_i)}{\partial t} + \frac{\partial}{\partial x_k}(\rho u_i u_k - \tau_{ik}) + \frac{\partial P}{\partial x_i} = S_i;\\
&\frac{\partial (\rho E)}{\partial t} + \frac{\partial}{\partial x_k}((\rho E + P)u_k + q_k - \tau_{ik} u_i) = S_k u_k + Q_H,
\end{aligned} \tag{1}$$

where u_i are the gas velocity vector components; ρ, P are the gas density and pressure; S_i are the external volumetric forces; E is the total energy per unit mass of gas; Q_H is the heat released in a unit volume of gas; τ_{ik} is the tensor of viscous shear stresses; q_i is the heat flow.

Tensor of viscous shear stresses is determined as follows:

$$\tau_{ik} = \mu \cdot \left(\frac{\partial u_i}{\partial x_j} + \frac{\partial u_j}{\partial x_i} - \frac{2}{3}\frac{\partial u_l}{\partial x_l}\delta_{ij}\right) - \frac{2}{3}\rho k \delta_{ij}, \tag{2}$$

where $\mu = \mu_l + \mu_t$ is the viscosity coefficient; μ_l is the molecular (dynamic) viscosity coefficient; μ_t is the turbulent viscosity coefficient; δ_{ij} is the Kronecker delta; k is the kinetic turbulence energy.

Certainly, the gas flow is turbulent. Obviously, the direct solution to three-dimensional unsteady DNS using spatial grids can be used to describe all significant flows, including spatiotemporal inhomogeneities. However, it is not less obvious that for its numerical implementation, it is necessary to use very small grids, where the nodes number should significantly increase with increasing Reynolds number.

As DNS requires three-dimensional unsteady calculation, the cost of the calculation is proportional to the total number of grid nodes, the number of time steps, and proportional to Re^3. This means that when the Reynolds number doubles, the costs increase by about an order of magnitude. Therefore, these methods are not used to calculate flows with complex geometry, and in practice, DNS is used only to calculate simple turbulent flows at low Reynolds numbers (about 103 and below).

Thus, as an alternative approach, the Reynolds-averaged method has now become the most widespread.

It is believed [7] that the average values of the pulsation components are zero, but the averaging from the multiplication of the pulsation components by each other is not zero. In the averaged equations of motion, additional terms (Reynolds stress) equal to $-\rho\overline{u_i' u_l'}$ appear, which describe the change in momentum caused by the interaction of turbulent velocity fluctuations.

To determine the Reynolds stresses, the Boussinesq hypothesis [7], which joins these stresses and the mean velocity gradients, is usually used:

$$-\rho\overline{u_i' u_l'} = \mu_T\left(\frac{\partial u_i}{\partial x_j} + \frac{\partial u_j}{\partial x_i}\right) - \frac{2}{3}\left(\rho k + \mu_T \frac{\partial u_i}{\partial x_i}\right)\delta_{ij} \tag{3}$$

The obtained equations describe the behavior of the averaged characteristics of turbulent flow, if the coefficients of viscosity and thermal conductivity are taken to be effective values equal to the sum of molecular (laminar dynamic) and turbulent viscosity and thermal conductivity, respectively:

$$\mu = \mu_l + \mu_T,\ \lambda = \lambda_l + \lambda_T \tag{4}$$

To determine the μ_T and λ_T, there are numerous semi-empirical theories of turbulence, which can be divided into algebraic and differential models. In this paper, the equation of the shear-stress transport (SST) model of turbulence is used [8], which shows high accuracy in the near-wall flows simulation.

To specify the turbulent viscosity value in this model, the following equation is used:

$$\mu_T = \frac{\rho a_1 k}{\max(a_1\omega;\, \Omega F_2)}, \tag{5}$$

where $F_2 = \tanh(\arg_2^2)$; $\arg_2 + \max(2\frac{\sqrt{k}}{0.09\omega y};\, \frac{500\nu}{y^2\omega})$ is the function equal to one for the boundary layer and zero for the free layers; $\Omega = (\partial u/\partial n)$ is the derivative of the flow velocity in the direction normal to the wall. To determine the kinetic energy and its dissipation, the following equation is used:

$$\begin{aligned}
&\frac{\partial \rho k}{\partial t} + \frac{\partial}{\partial x_i}(\rho u_i k) = \tau_{ij}\frac{\partial u_i}{\partial x_j} - \beta^*\rho\omega k + \frac{\partial}{\partial x_i}((\mu_l + \sigma_k\mu_t)\frac{\partial k}{\partial x_i});\\
&\frac{\partial \rho\omega}{\partial t} + \frac{\partial}{\partial x_i}(\rho u_i \omega) = \frac{\gamma\rho}{\mu_T}\tau_{ij}\frac{\partial v_i}{\partial x_j} - \beta\rho\omega^2 + \frac{\partial}{\partial x_i}((\mu_l + \sigma_\omega\mu_t)\frac{\partial \omega}{\partial x_i}) +\\
&+ 2\rho(1-F_1)\sigma_{\omega_2}\frac{1}{\omega}\frac{\partial k}{\partial x_j}\frac{\partial \omega}{\partial x_j},
\end{aligned} \tag{6}$$

where β, β^*, σ_k, σ_ω are the empirical constants, which are calculated by the formula $\varphi = F_1\varphi_1 + (1-F_1)\varphi_2 k - \varepsilon k - \omega$,

where φ_1, φ_2 are the corresponding empirical coefficients $k-\varepsilon$ and $k-\omega$ of turbulence models; F_1 is the function that acts as a switch between models so that near the wall $F_1 = 1$, and away from the surface $F_1 = 0$.

German scientist F. R. Menter was the first who proposed the formulation of the SST model from the condition of calculations stability [8], justifying the choice of the F_1 function in the form

$$F_1 = \tanh(\arg_1^4) \tag{7}$$

where $\arg_1 = \min[\max(\frac{\sqrt{k}}{0.09\omega y};\, \frac{500\nu}{y^2\omega});\, \frac{4\rho\sigma\omega_2 k}{CD_{k\omega}y^2}]$; y is the distance to the nearest wall.

$$CD_{k\omega} = \max(2\rho\sigma_{\omega_2}\frac{1}{\omega}\frac{\partial k}{\partial x_j}\frac{\partial \omega}{\partial x_j}, 10^{-20}). \tag{8}$$

3 Description of the Mathematical Models Used to Simulate the PMID Striker Movement

3.1 Determination of the Forces Acting on the Striker

Acceleration of the striker is a complex multifactorial process, which is significantly influenced by both the parameters of the gas environment and the conditions of gas leakage associated with the design features of the tool. As mentioned above, this process is described numerically using the system of Navier–Stokes equations, which is solved using FEM. Solving such a problem with complex spatial geometry requires large computational resources, which is enhanced by the need to rearrange the finite elements (FE) grid in real time during the calculation when its quality deteriorates. In this regard, two approaches are proposed to solve the problem of the PMID gas dynamics taking into account the movement of the striker:

– multiconfiguration approach in a flat axisymmetric setting;
– axisymmetric approach with the elementary sector selection and the use of the mechanism of the FE grid automatic rearrangement.

Acceleration of the striker is determined by the net force – the resultant of forces acting on the striker [9]:

$$R = P_3 - P_n - F_T, \tag{9}$$

where R is the resultant force; P_3 is the force developed by the gas expanding behind the striker; P_n is the force of air resistance in front of the striker; F_T is the force of friction of the striker against the barrel walls.

Sealing with O-rings has become widespread in hydraulic and pneumatic systems. The tightness in the seals of this type is achieved when there is no pressure, due to the previous (mounting) compression of rubber ring in the groove. Whenever the pressure in the system appears, the ring is further deformed, creating a dense contact with a sealed surface.

When performing design, calculation, research works and the construction of MM of various hydraulic and pneumatic devices, there are some difficulties in taking into account friction forces because of the lack of analytical dependencies for them. Known methods for determining friction are mainly based on tabular experimental data. In the work [9], it is recommended to calculate the friction forces in seals with rubber O-rings using the formula

$$F_T = q \cdot \pi \cdot D \tag{10}$$

where q is the specific friction force (force per unit length of contact of the O-ring with the moving surface); D is the diameter of the sealing surface.

The value of the specific friction force depends on the cross-sectional diameter of the ring d, the relative compression of the ring W, and the hardness of the O-ring material.

For the inertial forces, the striker was considered as a rigid body with a mass corresponding to the real mass of the striker, the boundary of which is assigned to the boundary conditions of the wall. During the development of the MM, a special 6 Degree of Freedom (6DOF) solver was connected, which calculates the position and orientation of the striker as a rigid body using the equations of motion. These equations describe six degrees of freedom: three translational and three rotational. In this case, the position of the body is determined by the three Euler angles and three translational coordinates [10].

When solving problems with deformed areas, the distortion of the FE grid leads to the appearance of the degenerate FE or significant deterioration of their quality. Periodic rearrangement of the FE grid for the computational domain is a very important part of the analysis, which contains significant displacements of the computational domain boundaries and deformation of the FE grid.

Therefore, in order to obtain an adequate result of the problem to be solved, the integration of the FE grid rearrangement cycle into the general problem solving cycle is applied.

As mentioned above, two approaches have been proposed to solve the PMID gas dynamics problem taking into account the striker motion.

3.2 Approach 1. Multiconfiguration Approach to Solving Problems with Moving Boundaries

The computational domain is a flat area that corresponds to the cross-section of the pneumo-impulse hammers with a plane passing through the axis of the symmetry (Fig. 1). The displacement of the striker under the pressure drop in cavities in front of and behind the striker was studied.

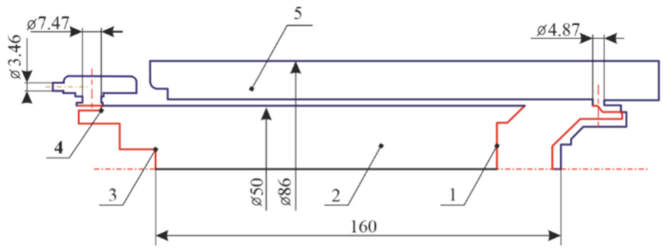

Fig. 1. Geometry of the computational domain with the striker (1), the barrel (2), the crimp (3), the quick release valve (4) and the receiver (5)

It is assumed that at the time before the opening of the relief valve, the air in the barrel and receiver was at the temperature of 300 K and the initial pressure of 0.5 MPa. The pressure of the external environment is taken to be equal to 0.1 MPa, the temperature is 300 K. It is assumed that the relief valve is opened in 0.01 s. The weight of the striker is 0.139 kg. The condition for stopping the calculation is the moment of contact of the striker and the crimp.

The simulation was performed for cases with different ratio of the striker V_x and the volume of the receiver V_p. The influence of the gas leakage conditions on the velocity and energy of the striker has also been studied. The multiconfigurational approach assumes the presence of several computational domain configurations depending on the striker position during the task performing. In this case, seven configurations were used, which corresponded to the stroke of the striker at 0.001, 0.008, 0.028, 0.058 and 0.088 m. Within a specific configuration, the FE calculation grid is deformed at a speed that is characteristic to the instantaneous velocity of the striker. Thus, switching to a new grid occurs automatically when the striker moves on the set distance. The maximum cells number of the FE grid was 15643.

The gas velocities distributions obtained from the simulation results, as well as the calculated striker velocities for different cases are shown in Figs. 2 and 3.

In Fig. 3, the computational domain was supplemented by a reflection relative to the axis of the symmetry for better clarity. Velocity and energy of the striker for cases with different V_x/V_p ratio is shown in Fig. 3 (a), with different conditions of gas leakage is shown in Fig. 3 (b).

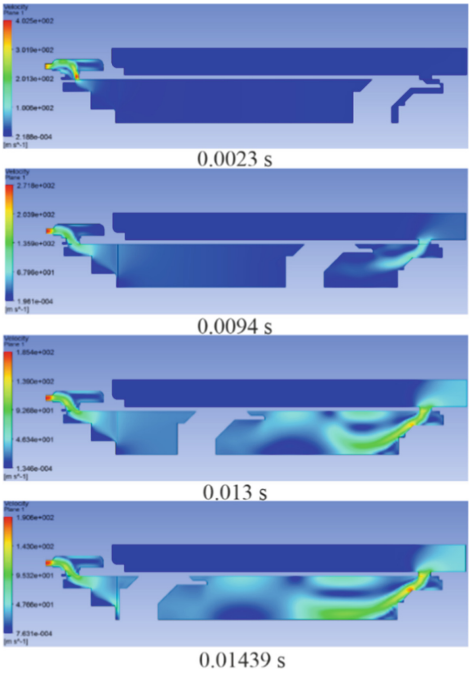

Fig. 2. Fields of gas flow velocities in different periods of time

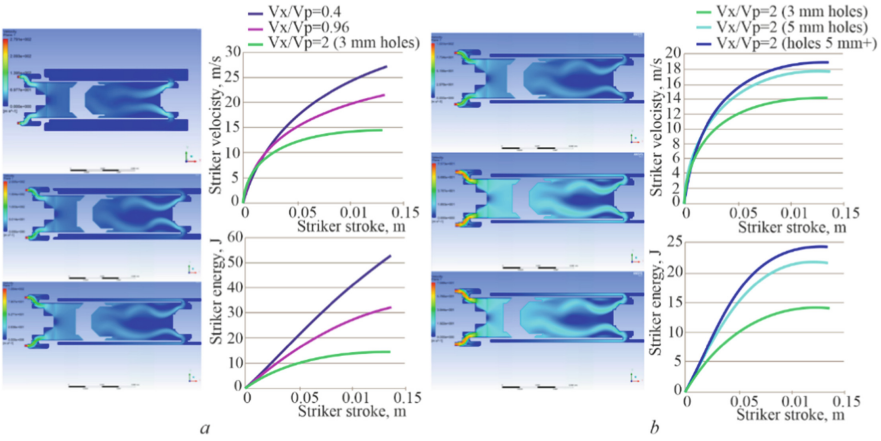

Fig. 3. Velocity and energy of the striker for cases: (a) with different V_x/V_p ratio; (b) with different conditions of gas leakage

The simulation results show that with the increasing V_x/V_p ratio, the velocity and energy of the striker decrease, and at the $V_x/V_p \geq 2$ the braking of the striker is happening. Thus, when the striker passes 0.13 m, which is equivalent to 2.7 d_s, its velocity reaches a peak value of 14 m/s, and then begins to decline. With the increasing diameter

of the outlets on the PIH-90 hammer front cover, the striker begins to brake when passing the distance of 0.135 m, but the maximum velocity reaches 19 m/s. A summary graph of the simulation results for different cases is shown in Fig. 4. The calculation time for each individual case was not more than 1 h depending on the size of the computational domain.

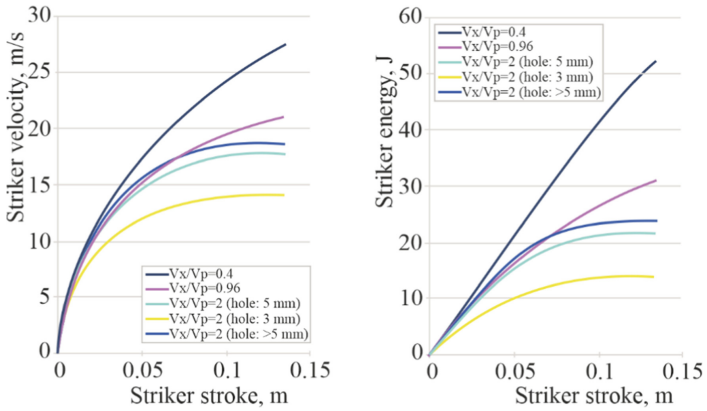

Fig. 4. Comparison of velocity and energy of the striker for different conditions

3.3 Approach 2. Axisymmetric Approach with the Elementary Sector Selection

The computational domain is a sector. To be able to build a sector with a regular placement of holes, the original geometry of the tool was changed to provide the same number of holes in the gas outlet areas on the front cover, the gas flow when opening the relief valve and the gas flow from the receiver into the cavity behind the striker. The holes size was recalculated in compliance with the holes cross-sectional area equivalence in the original and modified geometry of the tool.

The angle of the sector with one row of holes was 17.14°.

To compare the calculations performance, two computational domains were considered, which differed in the number of holes rows (see Fig. 5). The initial and boundary conditions are similar to the solution of the problem in 2D formulation.

To implement the formulated task, the mechanism of the FE grid automatic rearrangement was used, which is shown in Fig. 6.

When implementing this approach, the minimum angle of the FE grid element over the entire computational domain was chosen as a control parameter. The connection of the grid rearrangement cycle occurred when an element with an angle at the vertex less than 5° appeared in the computational domain. Then the grid was rearranged, and the calculation continued on the new grid, where, after interpolation of the results from the previous iteration, the initial conditions for further calculations were added.

The simulation results showed that the sector size does not affect the flow nature in the PMID channels.

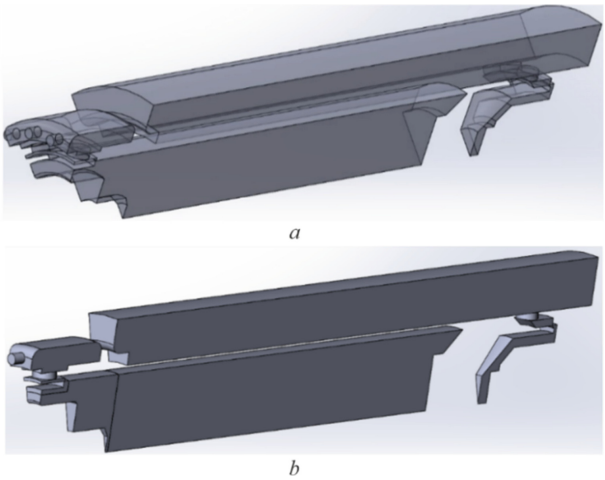

Fig. 5. Computational domain geometry in the form of an elementary sector, where three rows (a) and one row (b) are shown

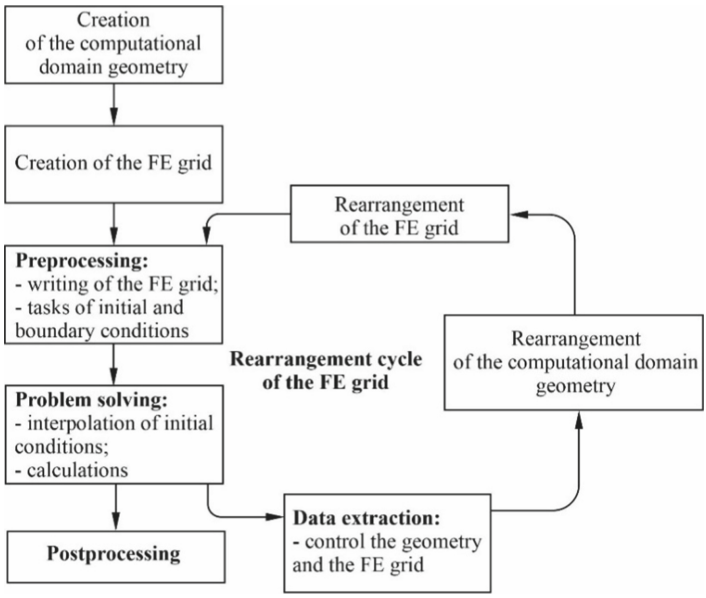

Fig. 6. Integration of the FE grid rearrangement cycle into the general problem solving cycle

The graph of the striker velocity change with its stroke increase for the cases with different sectors is shown in Fig. 7. The maximum relative error was 4%. At the same time, the calculation time was reduced from 13 to 6 h, which was due to a significant reduction in the FE grid cells number. Thus, for the sector with three rows of holes, the calculation grid consisted of 263,326 cells, and the sector with one row of holes consisted

of 102,359 cells. This confirmed the expediency of using a sector with a smaller angle to speed up the calculations.

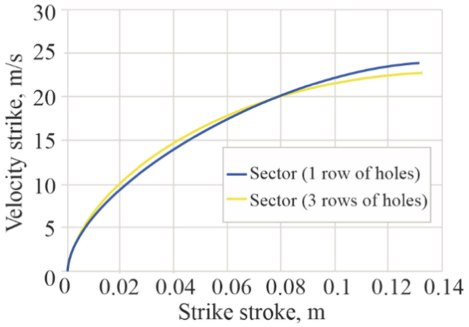

Fig. 7. Striker velocity comparison for different computational domain geometries

In order to verify the possibility of implementing the coherent problem of the PMID gas dynamics and the striker and crimp mechanics, the possibility to use the laminar flow in the gas dynamics calculations was verified (which was due to the solver limitations in the coherent problems solving). It is necessary to compare the crimp velocity obtained during the simulation with experimental data in this calculation in order to confirm the possibility of using the developed MM for designing a new PMID.

The comparison results are shown in Fig. 8 (a), according to which maximum relative error was 2% (for convenience, the figure shows the laminar flow part of the graph).

Figure 8 (b) shows the comparison of simulation results with theoretical data.

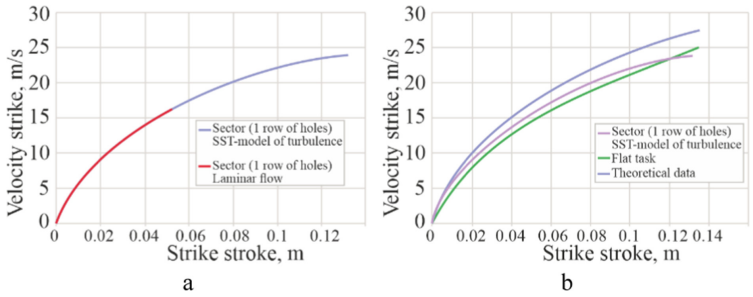

Fig. 8. Comparison of the turbulent and laminar flows (a) and comparison of the simulation results with known theoretical data (b)

The maximum error was 8% for a plain problem and 12% for a sector. The error is explained by a large number of assumptions taken in theoretical calculations. Thus, in work [11], the following assumptions were adopted:

– the process of gas expansion occurs not continuously, but discreetly, so the entire gas tract is divided into several sections and the pressure inside the section is considered a constant value for the entire section;

– the process is considered one-dimensional, and the inhomogeneity of the velocity field and losses at the boundaries and within the sections are taken into account using the coefficients of local and path losses;
– the interaction between the sections occurs according to the decay scheme of the initial gap;
– local sound speed is considered a constant value for all sections.

This leads to the inflated calculated values of the PMID energy parameters.

Considering the influence of the boundary layer on the energy parameters of the tool, it should be noted that the regular FE grid does not allow to accurately simulate the boundary layer near the walls. Simulation with the Free Slip and No Slip boundary conditions showed identical results. The striker velocity at the time of collision with the crimp was 33 m/s. The simulation was performed taking into account the supply of the receiver with compressed air with a pressure of 0.5 MPa.

Assuming the losses caused by gas inhibition near the walls, it was decided to improve the FE grid by creating prismatic layers (10 layers at a distance of 1 mm from the wall).

Solving the problem using the gas laminar flow model showed the limitations of this approach. At a distance of 0.125 m from the initial position of the striker (see Fig. 9), the calculation was stopped with the error of the Reynolds number value going outside the laminar flow model.

Fig. 9. Gas flows in the pneumo-impulse hammer channels

Thus, for a more accurate gas-dynamic calculation, it is necessary to apply the turbulence model, which would take into account the presence of a boundary layer under the walls. For this purpose, the SST model of turbulence was chosen.

According to the calculation results, the striker velocity at the time of contact with the crimp was 24 m/s.

According to the results of the numerous simulations using an improved grid, additional energy losses were revealed. Consequently, the striker velocity decreased by 9 m/s. The relative deviation was 27%.

Summary data for all calculation cases is shown in Fig. 10.

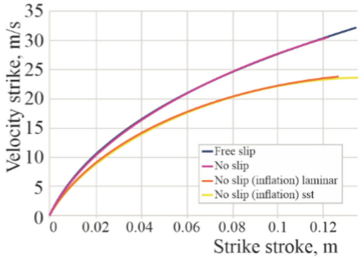

Fig. 10. Simulation results

A significant limitation of the ANSYS CFX system is inability to take into account the contact of solids. This significantly narrows the range of the system application and makes it impossible to solve the problem of structural-fluid interaction in a single computing environment. Therefore, it is necessary to use additional systems of structural analysis, which will lead to a significant increase of calculation time and to an additional error in data transmission between different packages.

4 Conclusions

The principles of creation and improvement of PMID were developed.

The direct problem of PMID design was solved using the results of gas-dynamic calculations of the devices energy parameters in the ANSYS CFX software package, which allow to determine the velocity and energy of the striker taking into account its mass characteristics, friction losses and design features of the device elements.

It is shown that increasing the V_x/V_p ratio from 0.4 to 2 leads to a decrease in the striker velocity from 28 to 14 m/s and in the blow energy from 52 to 14 J. At $V_x/V_p = 2$, the braking area appears after striker passes the distance equivalent to 2.7 d_s. Increasing the diameter of the holes at the outlet of the hammer front cover from 3 to 5 mm allows to increase the striker velocity from 14 to 19 m/s, and the blow energy from 14 to 24 J.

The simulation with different geometry of the computational domain was performed: two-dimensional formulation, a sector with three rows of holes and a sector with one row of holes. The calculation time for a sector with three rows of holes was 13 h; for a sector with one row of holes – 6 h; for a plane problem –1 h. The maximum relative error of the results in the case of using 2D geometry and the sector does not exceed 5%. Thus, for design calculations, it is expedient to use a 2D formulation, as it significantly reduces the calculation time. After completing the design, it is expedient to perform a test calculation, using the geometry in the form of a sector.

References

1. Krivtsov, V.S., Nechyporuk, N.V., Vorobiov, I.A., Voronko, V.V., Vorobiov, A.I.: Development of a technological process and a tool for impulse riveting of aviation parts made of carbon fiber. KhAI, Kharkov (2012)

2. Voronko, V.V., Vorobiov, I.A., Voronko, I.A., Kruglov, V.V.: Development of control systems for the pneumo-pulse energy unit for holes mandrelling of aviation parts as a robotic complex. Open Inf. Comput. Integr. Technol. (74), 88–98 (2016)
3. Krivtsov, V.S., Vorob'ev, Yu.A., Voron'ko, V.V.: Advanced devices for mandreling bores. Kuznechno-Shtampovochnoe Proizvodstvo (Obrabotka Metallov Davleniem) (12), 18–30 (2004)
4. Vorobiov, I.A.: The scientific basis for the creation of a complex of impulse technologies and equipment for the aggregate assembly of airframes (Doctoral dissertation) (Engineering). Kharkiv (2020)
5. Krivtsov, V.S., Voronko, V.V., Zaytsev, V.Ye.: Advanced prospects for development of aircraft assembly technology. Sci. Innov. **11**(3), 12–20 (2015). https://doi.org/10.15407/scin11.03.012
6. Garbaruk, A.V., Strelets, M., Shur, M.L.: Modeling of Turbulence in Calculations of Complex Flows. Publishing by Politechnic University, St. Petersburg (2012)
7. Plankovskyy, S., Shypul, O., Tsegelnyk, Ye., Tryfonov, O., Golovin, I.: Simulation of surface heating for arbitrary shape's moving bodies/sources by using R-functions. Acta Polytechnica **56**(6), 472–477 (2016). https://doi.org/10.14311/AP.2016.56.0472
8. Menter, F.R., Kuntz, M., Bender, R.: A scale-adaptive simulation model for turbulent flow predictions. In: 41st Aerospace Science Meeting & Exhibit, Nevada, Reno, 11 p. (2003)
9. Mitar, J., Šević, D., Karanovic, V., Beker, I., Dudić, S.: Increased efficiency of hydraulic systems through reliability theory and monitoring of system operating parameters. Strojniski Vestnik **584**(4), 281–288 (2011). https://doi.org/10.5545/sv-jme.2011.084
10. Plankovskyy, S., Tedorczyk, A., Shypul, O., Tryfonov, O., Brega, D.: Determination of detonable gas mixture heat fluxes at thermal deburring. Acta Polytechnica **59**(2), 162–169 (2019). https://doi.org/10.14311/AP.2019.59.0162
11. Encyclopedia of Mechanical Engineering XXL. http://mash-xxl.info/info/687955/. Accessed 09 Sept 2012